Romanian Reports in Physics, Vol. 68, No. 1, P. 230–240, 2016

DISPERSION RELATIONS OF STRAINED AND COMPLEX LIEB LATTICES BASED ON THE TIGHT-BINDING METHOD

YIQI ZHANG[1,*], XING LIU[1], MILIVOJ R. BELIĆ[2,†], WEIPING ZHONG[3], CHANGBIAO LI[1], HAIXIA CHEN[1], YANPENG ZHANG[1,‡]

[1]Key Laboratory for Physical Electronics and Devices of the Ministry of Education & Shaanxi Key Lab of Information Photonic Technique, Xi'an Jiaotong University, Xi'an 710049, China
[2]Science Program, Texas A&M University at Qatar, P. O. Box 23874 Doha, Qatar
[3]Department of Electronic and Information Engineering, Shunde Polytechnic, Shunde 528300, China
[*]zhangyiqi@mail.xjtu.edu.cn
[†]milivoj.belic@qatar.tamu.edu
[‡]ypzhang@mail.xjtu.edu.cn

Received June 16, 2015

Abstract. We investigate dispersion relations of strained complex Lieb lattices systematically, based on the tight-binding method with the nearest-neighbor approximation adopted. We find that there are edge states for strained Lieb lattices with solid edges, while there are no edge states for the pointy and pointy-solid edges. Different from honeycomb lattices, the $\mathcal{PT}$-symmetric Lieb lattices cannot be generated.

Key words: Lieb lattice, dispersion relation, complex lattice, edge state.

1. INTRODUCTION

Optical lattices are special photonic structures that can modulate light effectively and were much investigated in the past decades [1–6]. Recently, edge states of different kinds of lattices, with the corresponding boundaries, have attracted a lot of attention. Among different lattices, honeycomb lattices [7–15] and Lieb lattices [16–23] have excited a lot of interest. Photonic topological insulators with strange optical properties, based on the two kinds of lattices, have been reported in [24–26]. The reason that lattices exhibit such exotic optical properties lies in the existence of Dirac cones in the energy bands in the momentum space. The edge states that appear in the bulk band gap will spatially localize on the boundaries of strained lattices [7, 21, 27, 28] and will be robust against defects, due to the topological protection – thus possibly forming a topological insulator.

Lieb lattice, which is the face-centered square lattice, has three lattice sites in each unit cell. As reported previously [16–19], it displays a triply-denegerate diabolical point at which two conical bands and a flat band intersect. The flat band is a non-dispersive band and is topologically trivial [28], which corresponds to totally degenerate eigenstates. Since the states are degenerate, they are strongly correlated [29], and lead to enhanced light-matter interaction [30]. In addition to Lieb lattices,

flat bands are also reported in honeycomb lattices with inhomogeneous strains [31] or polarized monochromatic light irradiations [11], in kagome lattices [32, 33], square lattices [29], $\mathcal{T}_3$ optical lattices [34], etc. Similar to honeycomb lattices, Klein tunneling [17] and conical diffraction [19] are also demonstrated in Lieb lattices. Different from the honeycomb lattices, edge states of strained Lieb lattices are not reported before, to the best of our knowledge. Even though edge states of Lieb lattices are mentioned previously [18, 20, 21, 26, 28], they are not investigated in-depth.

It is known that if at the sites of the honeycomb lattice gain and loss are provided alternatively, the corresponding dispersion relation will be complex. However, the dispersion relation will be real again if the honeycomb lattice is artificially deformed. That is, the $\mathcal{PT}$-symmetric honeycomb lattices can be produced [35]. Similar to the honeycomb lattice, a Lieb lattice can also be made complex, but this possibility was not explored before. A question arises, can complex Lieb lattices also exhibit $\mathcal{PT}$-symmetric properties? Can strained Lieb lattices exhibit edge states? This paper will answer these questions.

For investigating the edge states, two methods are used. One is the nearest-neighbor method, which treats the system with exact diagonalization of the cylinder [7]. The other method is relating the presence of edge states to the geometrical phase (Zak's phase) of the bulk [36, 37]. In our theoretical analyses, nearest-neighbor tight-binding method is adopted, which is also applied in previous works [7, 28, 35].

The organization of the paper is as follows. In Sec. 2, we study the dispersion relation of the two-dimensional Lieb lattice, using the tight-binding method; in Sec. 3, we investigate the dispersion relation of strained Lieb lattices with different edges (solid, pointy, solid-pointy and zigzag boundaries) systematically; in Sec. 4, the dispersion relation of complex Lieb lattices is discussed in detail. We conclude the paper in Sec. 5.

2. TWO-DIMENSIONAL DISPERSION RELATION

A Lieb lattice is displayed in Fig. 1(a), in which the lattice sites in a dashed square form a unit cell. We assume that the hopping among lattice points only happens between the nearest-neighbor (NN) sites, as shown by the double-headed arrows. Therefore, the corresponding Hamiltonian can be written as

$$H_{\mathrm{TB}} = -t\sum_{m}\left[(f^{*}_{\mathbf{r}_m}g_{\mathbf{r}_m+\mathbf{e}_1} + f^{*}_{\mathbf{r}_m}g_{\mathbf{r}_m+\mathbf{e}_2} + f^{*}_{\mathbf{r}_m}h_{\mathbf{r}_m+\mathbf{e}_3} + f^{*}_{\mathbf{r}_m}h_{\mathbf{r}_m+\mathbf{e}_4})\right] + \mathrm{h.c.}, \tag{1}$$

where $f^{*}_{\mathbf{r}_m}$ is the creation operator on the mth lattice site, $\mathbf{r}_m$ is the position of the mth lattice site, t is the hopping strength, and the vectors $\mathbf{e}_1 = (-a/2, 0)$, $\mathbf{e}_2 = (a/2, 0)$, $\mathbf{e}_3 = (0, -a/2)$, $\mathbf{e}_4 = (0, a/2)$ are shown in Fig. 1(a). In real and momentum spaces,

we have the transform pairs

$$f_k = \frac{1}{\sqrt{N}} \sum_m f_{\mathbf{r}_m} \exp(i\mathbf{k}\cdot\mathbf{r}_m),\ f_{\mathbf{r}_m} = \frac{1}{\sqrt{N}} \sum_k f_k \exp(-i\mathbf{k}\cdot\mathbf{r}_m). \tag{2}$$

Plugging Eq. (2) into Eq. (1), one obtains

$$\begin{aligned} H_{\mathrm{TB}} = &-t\sum_k f_k^* g_k [\exp(-i\mathbf{k}\cdot\mathbf{e}_1) + \exp(-i\mathbf{k}\cdot\mathbf{e}_2)] \\ &-t\sum_k f_k g_k^* [\exp(i\mathbf{k}\cdot\mathbf{e}_1) + \exp(i\mathbf{k}\cdot\mathbf{e}_2)] \\ &-t\sum_k f_k^* h_k [\exp(-i\mathbf{k}\cdot\mathbf{e}_3) + \exp(-i\mathbf{k}\cdot\mathbf{e}_4)] \\ &-t\sum_k f_k h_k^* [\exp(i\mathbf{k}\cdot\mathbf{e}_3) + \exp(i\mathbf{k}\cdot\mathbf{e}_4)]. \end{aligned} \tag{3}$$

Equation (3) can also be rewritten as

$$H_{\mathrm{TB}} = \sum_k \begin{bmatrix} f_k^*, & g_k^*, & h_k^* \end{bmatrix} \mathcal{H} \begin{bmatrix} f_k \\ g_k \\ h_k \end{bmatrix} \tag{4}$$

with the Hamiltonian kernel

$$\mathcal{H} = -2t \begin{bmatrix} 0 & \cos\left(\frac{ak_x}{2}\right) & \cos\left(\frac{ak_y}{2}\right) \\ \cos\left(\frac{ak_x}{2}\right) & 0 & 0 \\ \cos\left(\frac{ak_y}{2}\right) & 0 & 0 \end{bmatrix}. \tag{5}$$

Therefore, one can solve Eq. (5) for the eigenvalues

$$\begin{aligned} \beta_1 &= 0, \\ \beta_{2,3} &= \pm 2t \sqrt{\cos^2\left(\frac{ak_x}{2}\right) + \cos^2\left(\frac{ak_y}{2}\right)}, \end{aligned} \tag{6}$$

which contribute to the dispersion relation. In Fig. 1(b), we display the dispersion relation in the first Brillouin zone with $a = 1$ (the corresponding $k_{x,y} \in [-\pi,\ \pi]$). Note that we take $a = 1$ throughout the paper. It is clear that there is a flat band and two symmetric conical bands about the flat band; such symmetry is known as the particle-hole symmetry [19–21]. The two conical bands form a Dirac point, located at one corner of the first Brillouin zone and intersected by the flat band, as shown in Fig. 1(c), which is the zoomed region marked by the ellipse in Fig. 1(b).

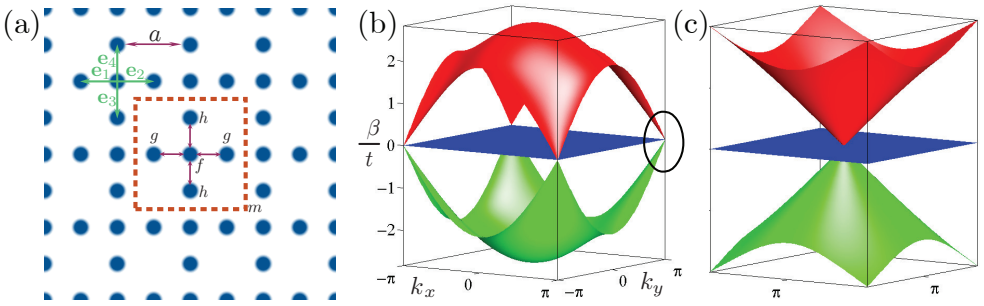

Fig. 1 – (a) Lieb lattice. (b) Dispersion relation in the first Brillouin zone. (c) Zoomed region marked with an ellipse in (b).

3. DISPERSION RELATIONS OF STRAINED LIEB LATTICES

Honeycomb lattice with bearded, zigzag, bearded-zigzag, and armchair boundaries can be strained [7, 12], which will lead to different dispersion relations. Similar to honeycomb lattice, a strained Lieb lattice can also have different boundaries, such as solid, pointy, solid-pointy, zigzag boundaries, etc. Therefore, different strained Lieb lattices may also possess different dispersion relations. In this section we present a thorough discussion on the dispersion relations of strained Lieb lattices with different boundaries.

3.1. SOLID EDGES

A Lieb lattice with solid edges is shown in Fig. 2(a), in which we mark off a unit cell with a rectangle. For convenience, we only show one layer, i.e. $n = 1$. According to the NN approximation, the Hamiltonian can be written as

$$\begin{aligned} H_{\text{straight}} = &-t\sum_m \left[f^*_{m1}(f'_{m2}+f_{m2})+f^*_{m2}(f_{m1}+f''_{m1}+f_{m3})\right] \\ &-t\sum_m \left[f^*_{m3}(f_{m2}+f_{m5})+f^*_{m4}(f'_{m5}+f_{m5})\right] \\ &-t\sum_m f^*_{m5}(f_{m3}+f_{m4}+f''_{m4}). \end{aligned} \tag{7}$$

In the momentum space, Eq. (7) can be written as

$$H_{\text{TB}} = \sum_k \left[f^*_{m1},\quad f^*_{m2},\quad f^*_{m3},\quad f^*_{m4},\quad f^*_{m5}\right]\mathcal{H}\begin{bmatrix} f_{m1} \\ f_{m2} \\ f_{m3} \\ f_{m4} \\ f_{m5} \end{bmatrix}, \tag{8}$$

in which the corresponding Hamiltonian kernel is

$$\mathcal{H} = -2t \begin{bmatrix} 0 & \cos\left(\frac{k_x}{2}\right) & 0 & 0 & 0 \\ \cos\left(\frac{k_x}{2}\right) & 0 & \frac{1}{2} & 0 & 0 \\ 0 & \frac{1}{2} & 0 & 0 & \frac{1}{2} \\ 0 & 0 & 0 & 0 & \cos\left(\frac{k_x}{2}\right) \\ 0 & 0 & \frac{1}{2} & \cos\left(\frac{k_x}{2}\right) & 0 \end{bmatrix}. \tag{9}$$

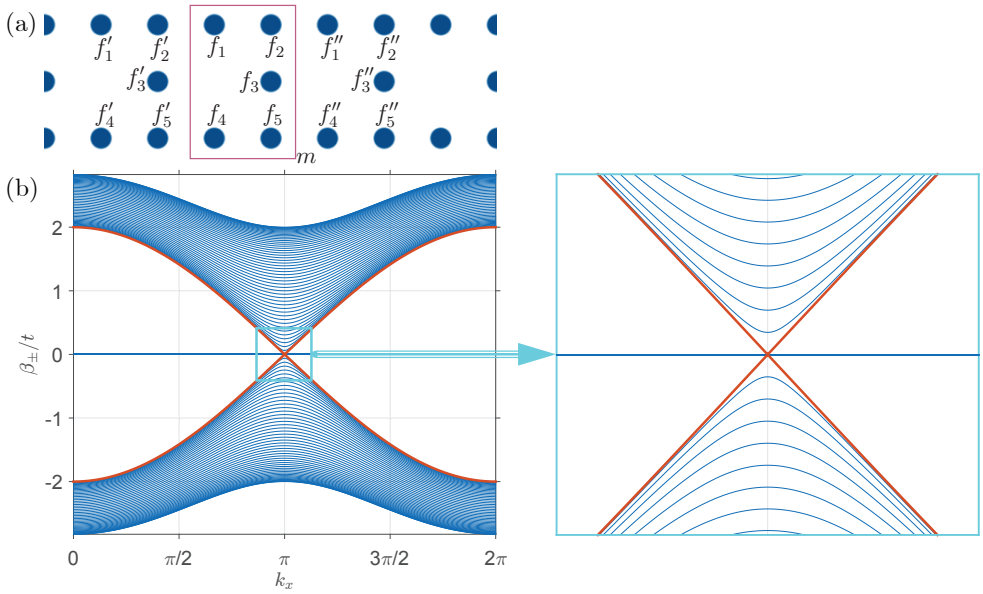

Fig. 2 – (a) Strained one-layer Lieb lattice with solid edges. The sites in the square compose a unit cell. (b) Left panel: corresponding band structure with $k_x \in [0,\ 2\pi]$ and $n = 50$. Right panel: a magnified view of the region shown in the left panel by a box.

It is clear that the Hamiltonian kernel is a 5×5 matrix, and the size of the matrix for any n can be induced to be $(2+3n) \times (2+3n)$. In Fig. 2(b), we show the band structure of a 50-layer Lieb lattice with two solid edges in $k_x \in [0,\ 2\pi]$. Even though the band structure is similar to those of a bearded honeycomb lattice [7, 10, 12], there is no degenerate band in the energy spectrum (the point at $\beta = 0$ is from the flat band). However, between the bulk band and the flat band, there are two states which fill the band gap. A magnified view of the region in left panel shows the states more clearly – they connect the bulk band and the flat band. These are the edge states corresponding to the strained Lieb lattice with solid edges.

3.2. POINTY EDGES

A Lieb lattice with pointy edges is exhibited in Fig. 3(a), in which the unit cell is also marked by a rectangle. The corresponding Hamiltonian in the momentum space can be written as

$$H_{\mathrm{TB}} = \sum_{k} \begin{bmatrix} f^*_{m1}, & f^*_{m2}, & f^*_{m3}, & f^*_{m4} \end{bmatrix} \mathcal{H} \begin{bmatrix} f_{m1} \\ f_{m2} \\ f_{m3} \\ f_{m4} \end{bmatrix}, \tag{10}$$

with

$$\mathcal{H} = -2t \begin{bmatrix} 0 & 0 & \frac{1}{2} & 0 \\ 0 & 0 & \cos\left(\frac{k_x}{2}\right) & 0 \\ \frac{1}{2} & \cos\left(\frac{k_x}{2}\right) & 0 & \frac{1}{2} \\ 0 & 0 & \frac{1}{2} & 0 \end{bmatrix}. \tag{11}$$

The dispersion relation of this strained Lieb lattice can be obtained from Eq. (11), and the results are displayed in Fig. 3(b), in which there is a band gap between the flat and the upper (bottom) bands. One can clearly see that there is no edge state in the band gap.

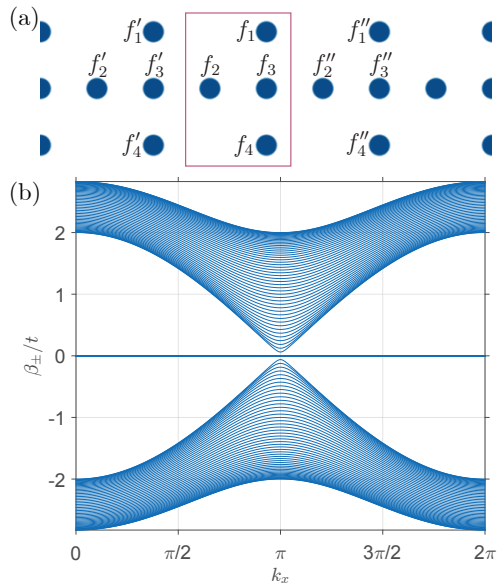

Fig. 3 – Strained Lieb lattice with pointy edges. Figure setup is similar to Fig. 2.

3.3. SOLID-POINTY EDGES

The Lieb lattice can also be strained with hybrid boundaries, as shown in Fig. 4(a) – one edge is solid and the other is pointy. The corresponding band structure can be obtained as before and is displayed in Fig. 4(b), which is similar to those displayed in Fig. 3. Therefore, there are still no edge states in this case.

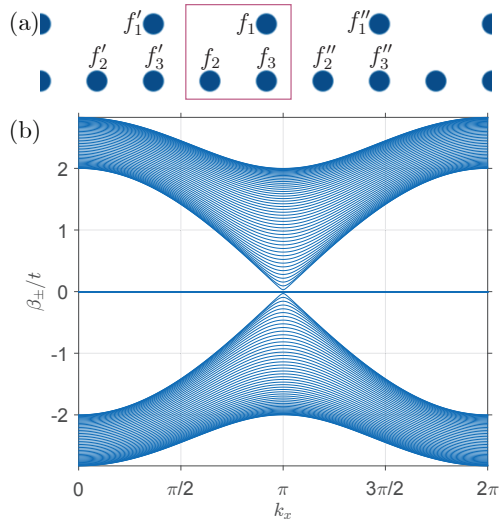

Fig. 4 – Strained Lieb lattice with solid-pointy edges. Figure setup is as in Fig. 3.

4. COMPLEX LIEB LATTICES

In the above section, we have theoretically investigated the dispersion relations of strained Lieb lattices with different edges. Similar to honeycomb waveguides [35], Lieb waveguides can also be made complex. Since there are three sites in each unit cell of Lieb lattice, we will assume that one waveguide exhibits gain, and the other two loss.

The structure of a complex Lieb waveguide lattice with alternating gain and loss is displayed in Fig. 5(a). Considering arrangement in the figure and according to the tight-binding model, the dynamics of the system can be described by

$$\begin{aligned} i\partial_z f_{\mathbf{r}_m} &= -\Delta f_{\mathbf{r}_m} - i\gamma f_{\mathbf{r}_m} + t(c g_{\mathbf{r}_m+\mathbf{e}_1} + g_{\mathbf{r}_m+\mathbf{e}_2} + h_{\mathbf{r}_m+\mathbf{e}_3} + h_{\mathbf{r}_m+\mathbf{e}_4}), \\ i\partial_z g_{\mathbf{r}_m} &= +\Delta g_{\mathbf{r}_m} + i\gamma g_{\mathbf{r}_m} + t(f_{\mathbf{r}_m+\mathbf{e}_1} + c f_{\mathbf{r}_m+\mathbf{e}_2}), \\ i\partial_z h_{\mathbf{r}_m} &= +\Delta h_{\mathbf{r}_m} + i\gamma h_{\mathbf{r}_m} + t(f_{\mathbf{r}_m+\mathbf{e}_3} + f_{\mathbf{r}_m+\mathbf{e}_4}), \end{aligned} \tag{12}$$

where γ describes the gain or loss of the waveguide, c is the deforming coefficient

of the lattice [8, 35], and Δ is the detuning in the effective index between adjacent waveguides.

We are looking for the solutions of the form:

$$\begin{aligned} f_{\mathbf{r}_m} =& F\exp[i(\beta z + mk_x + nk_y)], \\ g_{\mathbf{r}_m} =& G\exp[i(\beta z + mk_x + nk_y)], \\ h_{\mathbf{r}_m} =& H\exp[i(\beta z + mk_x + nk_y)] \end{aligned}$$

of Eq. (12). Here, F, G, and H are the amplitudes. Therefore, one obtains an eigenvalue problem

$$\mathcal{M}\begin{bmatrix} F \\ G \\ H \end{bmatrix} = \beta \begin{bmatrix} F \\ G \\ H \end{bmatrix}, \tag{13}$$

where $\mathcal{M}$ is the matrix

$$\begin{bmatrix} \Delta + i\gamma & -t\left[c\exp\left(i\frac{k_x}{2}\right) + \exp\left(-i\frac{k_x}{2}\right)\right] & -2t\cos\left(\frac{k_y}{2}\right) \\ -t\left[c\exp\left(-i\frac{k_x}{2}\right) + \exp\left(i\frac{k_x}{2}\right)\right] & -(\Delta + i\gamma) & 0 \\ -2t\cos\left(\frac{k_y}{2}\right) & 0 & -(\Delta + i\gamma) \end{bmatrix}. \tag{14}$$

The corresponding dispersion relation can be calculated as

$$\begin{aligned} \beta_1 =& -(\Delta + i\gamma), \\ \beta_{2,3} =& \pm\sqrt{\Delta^2 - \gamma^2 + 2i\gamma\Delta + t^2(c-1)^2 + 4ct^2\cos^2\left(\frac{k_x}{2}\right) + 4t^2\cos^2\left(\frac{k_y}{2}\right)}. \end{aligned} \tag{15}$$

Clearly, Eq. (15) is the same as Eq. (6) if $\Delta = \gamma = 0$ and $c = 1$, so that the dispersion relation is as in Fig. 1(b). If $\gamma = 0$ and $c = 1$, the eigenvalues are all real and the dispersion relation is displayed in Fig. 5(b) ($\Delta = 0.2$ for this case). In this case, the triply-degenerate diabolic point disappears. Instead, a band gap appears between one conical band and the flat band. While if $\Delta = 0$, $c = 1$ and $\gamma \neq 0$, the eigenvalues are complex. In Figs. 5(c) and 5(d), we show the real and imaginary parts of the dispersion relation with $\gamma = 0.5$, which is quite similar to the one of the complex honeycomb lattice [35]. As demonstrated previously [35], lattice deformation may lead to completely real eigenvalues even though the lattice is complex. In other words, there may exist the $\mathcal{PT}$-symmetric lattice.

Here, we also deform the complex Lieb lattice and investigate the corresponding dispersion relation. According to Eq. (15), when $\Delta = 0$ and if $0 < c \leq (1 - \gamma/t)$ or $c \geq (1 + \gamma/t)$, $\beta_{2,3}$ will be real. However, the flat band β_1 is always complex, be-

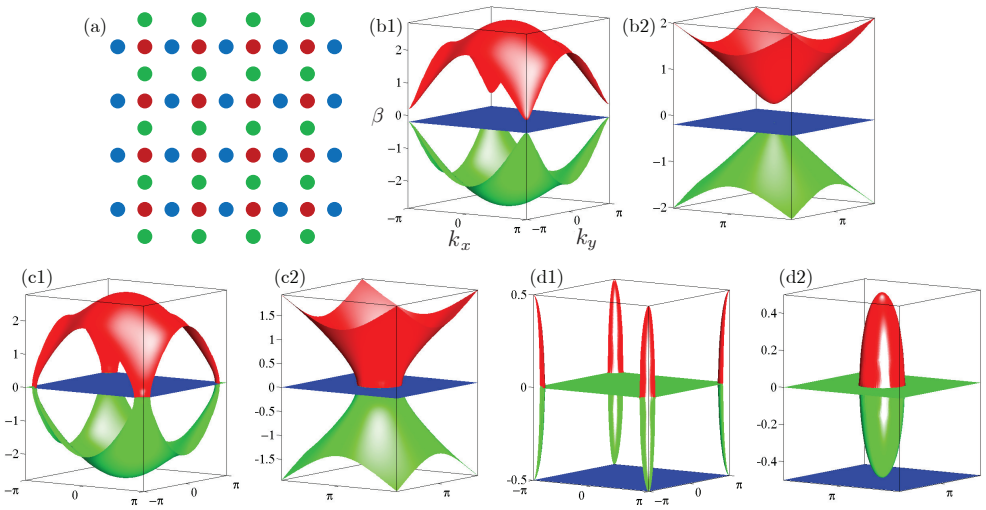

Fig. 5 – (a) Complex Lieb lattice. Each point represents a waveguide. The red waveguides exhibit gain, while the other two kinds exhibit loss. (b1) Dispersion relation with $\Delta = 0.2$ and $\gamma = 0$. (b2) A magnified view of the dispersion relation around a corner of the first Brillouin zone. (c) and (d) Figure setup is as in (b), but for the real and imaginary parts, for $\Delta = 0$ and $\gamma = 0.5$, respectively. For all the cases, $c = 1$.

cause it cannot be adjusted by the deforming coefficient c. Since the eigenvalues are always complex, there exists no $\mathcal{PT}$-symmetric strained Lieb lattice. Interestingly, the triply-degenerate diabolic point will reappear in the real parts of the dispersion relation if $c = 1 - \gamma/t$ or $c = 1 + \gamma/t$. For other cases with $0 < c < (1 - \gamma/t)$ or $c > (1 + \gamma/t)$, there is no degenerate diabolic point. No matter what the value of c is, the particle-hole symmetry holds true in the real part of the dispersion relation if $\Delta = 0$.

5. CONCLUSION

In summary, we have investigated the dispersion relations of strained and complex Lieb lattices. We find that there exist no edge states in the strained Lieb lattices with pointy and pointy-solid edges. However, for the case with solid edges, there are edge states. Concerning complex Lieb lattices, the $\mathcal{PT}$-symmetric Lieb lattices cannot be obtained either, because the flat band is not affected by the deforming coefficient and is always complex, even though the imaginary eigenvalues of the top and bottom bands can be eliminated. This investigation will help in understanding better the dispersion relations of strained Lieb lattices with different edges and complex Lieb lattices, and guide researchers to choose right structures in trying to fabricate

topological insulators.

Acknowledgements. This work was supported by the 973 Program (2012CB921804), KSTIT of Shaanxi province (2014KCT–10), NSFC (11474228, 61308015), CPSF (2014T70923, 2012M521773), and the Qatar National Research Fund NPRP 6–021–1–005 project. Qatar National Research Fund is a member of the Qatar Foundation.

REFERENCES

1. F. Lederer, G. I. Stegeman, D. N. Christodoulides, G. Assanto, M. Segev, and Y. Silberberg, Phys. Rep. **463**(1–3), 1–126 (2008).
2. S. Longhi, Laser Photon. Rev. **3**(3), 243–261 (2009).
3. I. L. Garanovich, S. Longhi, A. A. Sukhorukov, and Y. S. Kivshar, Phys. Rep. **518**(1–2), 1–79 (2012).
4. Y. V. Kartashov, B. A. Malomed, and L. Torner, Rev. Mod. Phys. **83**(1), 247–305 (2011).
5. Y. Q. Zhang, M. R. Belić, W. P. Zhong, F. Wen, Y. Guo, Y. Guo, K. Q. Lu, and Y. P. Zhang, J. Opt. **17**(4), 045606 (2015).
6. V. S. Bagnato, D. J. Frantzeskakis, P. G. Kevrekidis, B. A. Malomed, and D. Mihalache, Rom. Rep. Phys. **67**(1), 5–50 (2015).
7. M. Kohmoto and Y. Hasegawa, Phys. Rev. B **76**, 205402 (2007).
8. O. Bahat-Treidel, O. Peleg, M. Grobman, N. Shapira, M. Segev, and T. Pereg-Barnea, Phys. Rev. Lett. **104**, 063901 (2010).
9. K. K. Gomes, W. Mar, W. Ko, F. Guinea, and H. C. Manoharan, Nature **483**, 306–310 (2012).
10. M. C. Rechtsman, Y. Plotnik, J. M. Zeuner, D. Song, Z. Chen, A. Szameit, and M. Segev, Phys. Rev. Lett. **111**, 103901 (2013).
11. A. Crespi, G. Corrielli, G. D. Valle, R. Osellame, and S. Longhi, New J. Phys. **15**(1), 013012 (2013).
12. Y. Plotnik *et al.*, Nat. Mater. **13**(1), 57–62 (2014).
13. M. Bellec, U. Kuhl, G. Montambaux, and F. Mortessagne, New J. Phys. **16**(11), 113023 (2014).
14. Y. Q. Zhang, Z. K. Wu, M. Belić, H. B. Zheng, Z. G. Wang, M. Xiao, and Y. P. Zhang, Laser Photonics Rev. **9**(3), 331–338 (2015).
15. H.-S. Tao, W. Wu, Y.-H. Chen, and W.-M. Liu, Rom. Rep. Phys. **67**(1), 187–206 (2015).
16. V. Apaja, M. Hyrkäs, and M. Manninen, Phys. Rev. A **82**, 041402 (2010).
17. R. Shen, L. B. Shao, B. Wang, and D. Y. Xing, Phys. Rev. B **81**, 041410 (2010).
18. N. Goldman, D. F. Urban, and D. Bercioux, Phys. Rev. A **83**, 063601 (2011).
19. D. Leykam, O. Bahat-Treidel, and A. S. Desyatnikov, Phys. Rev. A **86**, 031805 (2012).
20. M. Niţă, B. Ostahie, and A. Aldea, Phys. Rev. B **87**, 125428 (2013).
21. D. Guzmán-Silva, C. Mejía-Cortés, M. A. Bandres, M. C. Rechtsman, S. Weimann, S. Nolte, M. Segev, A. Szameit, and R. A. Vicencio, New J. Phys. **16**(6), 063061 (2014).
22. R. A. Vicencio, C. Cantillano, L. Morales-Inostroza, B. Real, C. Mejía-Cortés, S. Weimann, A. Szameit, and M. I. Molina, Phys. Rev. Lett. **114**, 245503 (2015).
23. S. Mukherjee, A. Spracklen, D. Choudhury, N. Goldman, P. Öhberg, E. Andersson, and R. R. Thomson, Phys. Rev. Lett. **114**, 245504 (2015).
24. M. C. Rechtsman, J. M. Zeuner, Y. Plotnik, Y. Lumer, D. Podolsky, F. Dreisow, S. Nolte, M. Segev, and A. Szameit, Nature **496**(7444), 196–200 (2013).
25. G. Q. Liang and Y. D. Chong, Phys. Rev. Lett. **110**, 203904 (2013).

26. M. A. Bandres, M. Rechtsman, A. Szameit, and M. Segev, CLEO: 2014, p. FF2D.3 (2014).
27. K.-I. Imura, A. Yamakage, S. Mao, A. Hotta, and Y. Kuramoto, Phys. Rev. B **82**, 085118 (2010).
28. C. Weeks and M. Franz, Phys. Rev. B **82**, 085310 (2010).
29. K. Sun, Z. Gu, H. Katsura, and S. Das Sarma, Phys. Rev. Lett. **106**, 236803 (2011).
30. Z. Wang, Y. Chong, J. D. Joannopoulos, and M. Soljacic, Nature **461**, 772–775 (2009).
31. M. C. Rechtsman, J. M. Zeuner, A. Tünnermann, S. Nolte, M. Segev, and A. Szameit, Nat. Photon. **7**(2), 153–158 (2013).
32. S. Deng, A. Simon, and J. Köhler, J. Solid State Chem. **176**(2), 412–416 (2003).
33. S. Miyahara, K. Kubo, H. Ono, Y. Shimomura, and N. Furukawa, J. Phys. Soc. Jap. **74**(7), 1918–1921 (2005).
34. D. Bercioux, D. F. Urban, H. Grabert, and W. Häusler, Phys. Rev. A **80**, 063603 (2009).
35. A. Szameit, M. C. Rechtsman, O. Bahat-Treidel, and M. Segev, Phys. Rev. A **84**, 021806 (2011).
36. S. Ryu and Y. Hatsugai, Phys. Rev. Lett. **89**, 077002 (2002).
37. P. Delplace, D. Ullmo, and G. Montambaux, Phys. Rev. B **84**, 195452 (2011).